

The behavior of tapered one-way continuous two-span reinforced concrete slabs under repeated load

Fatima Mseer ¹, Nameer Alwash ²

¹ College of Engineering, University of Babylon, Iraq

² College of Engineering, University of Babylon, Iraq

ABSTRACT

The scope of this study is to look at the effect of supplying a non-prismatic cross-section on the flexural strength of one-way continuous slabs reinforced concrete (RC) with two spans under repeated load. The research aims to study the ability of non-prismatic slabs to increase flexural stiffness which leads to saving construction costs. For this purpose, experimental investigations were carried out; the work consisted of fabrication and testing six two-span RC slabs with the same volume of concrete. Two of them were prismatic with a constant depth, while all the others were non-prismatic with tapered cross-sections having varying depth. Prismatic slabs were stiffer than non-prismatic slabs in all support settings, according to the findings. It is found that providing a tapered slab with a positive or a negative haunch has an insignificant effect on the bearing capacity for a prismatic slab. On the other hand, the tapered slab led to increase the deflection at service load compared to the prismatic slab.

Keywords: Non prismatic; Repeated load; Slab; One way; Two span

Corresponding Author:

Nameer Alwash
College of Engineering, University of Babylon
Hilla, Babil, Iraq
eng.nameer.abdul@uobabylon.edu.iq

1. Introduction

Non-prismatic members are members with non-constant cross-sections along their length. Because the structural engineering techniques were improved, non-prismatic members are widely utilized in many structures including buildings and bridges [1]–[3]. Through material and structural member redistribution (tapering), architects and structural engineers can create and implement unique aesthetic architectural designations, as well as seek ideal low weight - high strength systems [4]–[6]. Recently, the impact of utilizing non-prismatic cross-section on the behavior of reinforced concrete (RC) structural components have been extensively studied. Researchers mostly focused on the tapered cross-section of RC beams [7]–[11]. When used to replace equal strength prismatic sections, these beams can reduce steel and concrete consumption (see Figure 1).

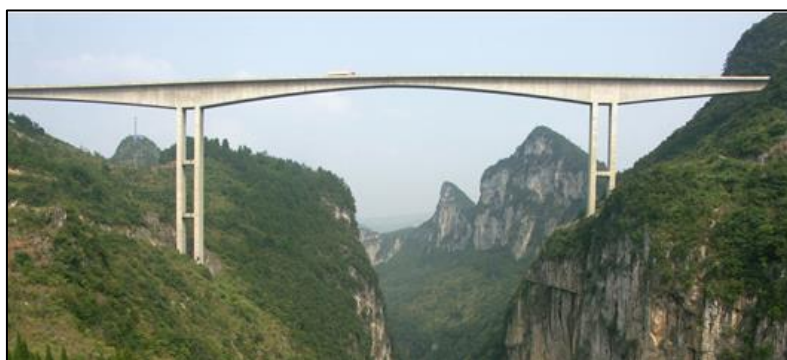


Figure 1. This is a figure. schemes follow the same formatting

Al-Shaarbaf et al., [12] explored the structural behaviour of voided slab strips built of regular and high strength self-compacted concrete (SCC) under repetitive load. The experiments were conducted using 10 one-way simply supported slabs that were subjected to monotonic and repetitive loads. According to one of their findings, the flexural failure mechanism of the specimens tested under repeated stress was identical to that of comparable specimens tested under monotonic load.

Toshniwal, [13] examined the mistakes that engineers make when performing cross-sectional analysis on non-prismatic bridge decks in practice. For an existing bridge deck that is the Wolweg Bridge in the Netherlands, the inaccuracy in cross-section findings for several models is computed. As illustrated in Figure 2, the bridge has two decks, each with three spans. The end decks are 10.5 meters long, while the main deck is 13 meters long. To boost the shear capacity, a tapered part is supplied at the middle support. In the southern half of the deck, where the study is centered, the width is 20.8 m.

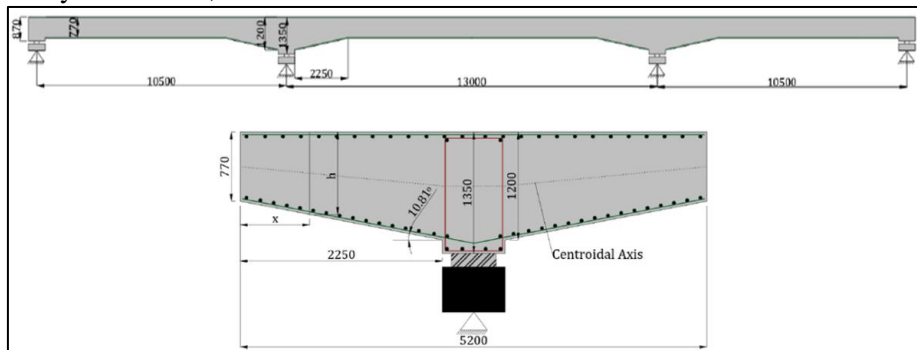


Figure 2. Deck dimensions and tapered section of the deck [6]

Engineers make many mistakes while doing cross-sectional analysis of haunched concrete bridges, according to Toshniwal [13], owing to the non-linear layout of the centroidal axis. Toshniwal [13] modified the haunched decks to make the centroidal axis remains linear while using the same volume of concrete as seen in Figure 3. The author discovered that this modification has no effect on the deck's shear capacity or bending moment resistance although these results were obtained at the ultimate limit state (ULS), and structural behavior at the serviceability limit state may differ (SLS).

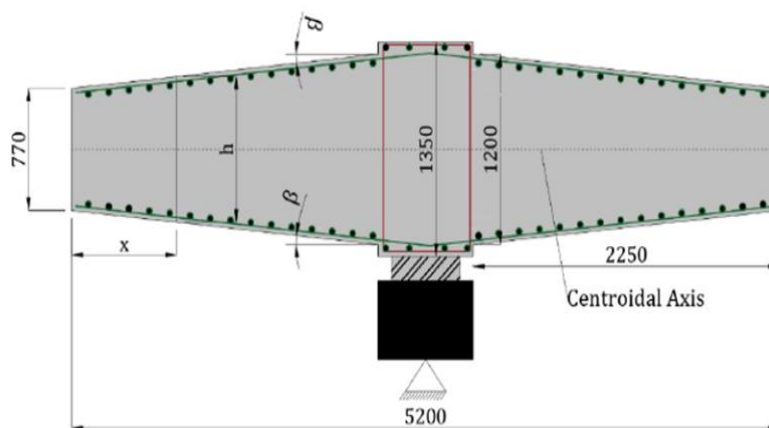


Figure 3. Modified tapered section of the deck [13]

It is well known from the literature mentioned above that there is a lack of knowledge concerning the effect of providing a non-prismatic cross-section on the strength and flexural behavior of reinforced concrete one-way slabs [14]–[17].

2. Experimental program

In this research, six RC one-way slabs were built and examined; two of them with prismatic cross-section and four slabs with different tapering configurations. The variables adopted in this research included:

1. The influence of tapering configuration on the behavior of continuous non-prismatic slabs under repeated load.
2. The behavior of slabs with different types of ending supports under repeated load.

The experimental program is described in detail in the parts below:

1.1. Materials properties

The attributes of the materials utilized in this investigation were determined in the laboratory. To guarantee that all the slabs tested have almost the same compressive strength, the samples were built and cured under the same settings. All slabs were produced with ordinary Portland cement, sand (maximum size is 4.75mm), and gravel (maximum size is 14mm). The concrete mix ratios (by weight) utilized in this investigation are shown in Table 1. Compressive and splitting tensile strength were measured using a compression testing machine. These two tests were performed on cylindrical concrete specimens of 300mm high and 150mm diameter. At 28 days, the average concrete splitting tensile and compressive strength were 3.28 MPa and 35.2 MPa, respectively. The results of a direct tensile test which has been conducted on three samples of $\varnothing 8$ mm diameter deformed steel bar was 550 MPa and 678 MPa for the yield and tensile strengths, respectively.

Table 1. Mixture Properties for the chosen concrete mixing

Material	The Selected Concrete Mix
Water/Cement proportion	0.3
Superplasticizer Sika VisoCrete® 5930-L (Liter)	4.5
Cement (Kg/m^3)	450
Fine aggregates (Kg/m^3)	765
Coarse aggregates (Kg/m^3)	1035

1.2. Description of specimens

All slabs were 3*0.5 meters using various depths with two equal spans of 1.3 meters. They were tested with two-point line loads, one in the center of each span until they failed. Each slab received 3 $\varnothing 8$ mm longitudinal steel reinforcement at the top and bottom, as well as $\varnothing 8$ mm transverse steel reinforcement every 200 mm at the top and bottom of the short direction. The clear concrete cover had a thickness of 20 mm. The six slabs tested in this investigation were divided into two series based on the type of support. The first series consists of three slabs that are simply supported. One of them was prismatic, with a constant depth of 100 mm, and served as the series' reference slab (S1 specimen). The other two slabs, on the other hand, were non-prismatic with tapered cross-sections of variable depth. One of these two slabs had a positive haunch of 130 mm at the center of each span and 70 mm at the supports (S2 specimen). The other slab contains a negative haunch of 70 mm in depth at the middle and 130 mm at the supports (S3 specimen). The second series consists of three slabs with fixed-end supports having the same size and characteristics as the first series example. Figures 4 and 5 show examples of the first and second series of these slabs in terms of geometry, reinforcement, and tapering arrangement, respectively.

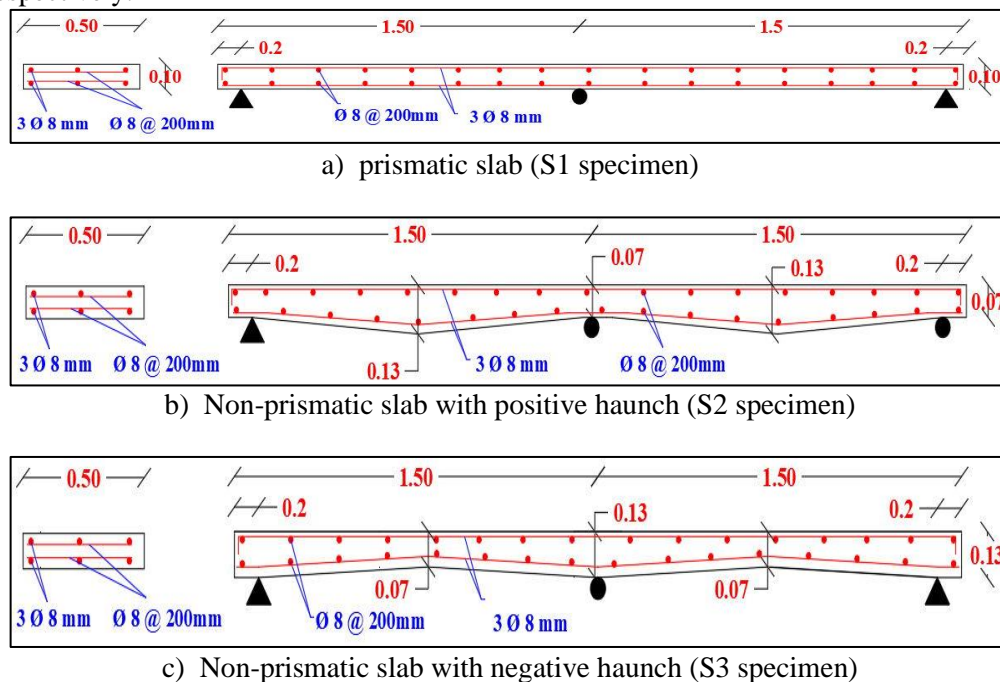


Figure 4. Geometric and reinforcement details for simply supported two-span slabs

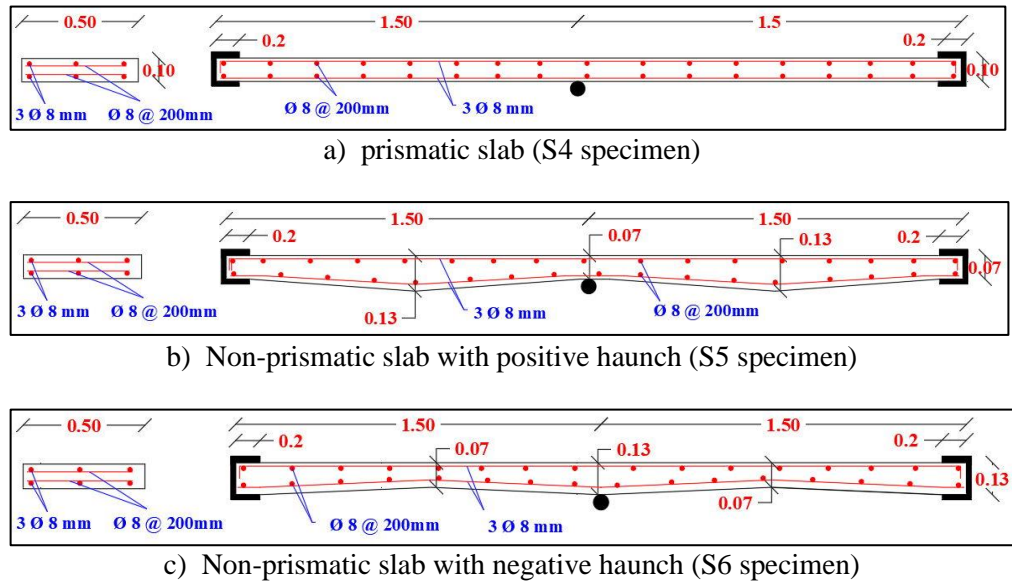


Figure 5. Geometric and reinforcement details for fixed end support two-span slabs

2. Test setup

At Babylon University's Structural Engineering Laboratory, RC slabs were subjected to repeated loads till failure using a hydraulic testing machine with a capacity of 600 kN. Each slab was supported in its way. A spreader steel beam was used to apply a one-line load to the tested slab in the center of each span. To avoid local concrete crushing, bearing plates were employed at the supports and loading points. The machine utilized in the test is shown in full in Figure 6.

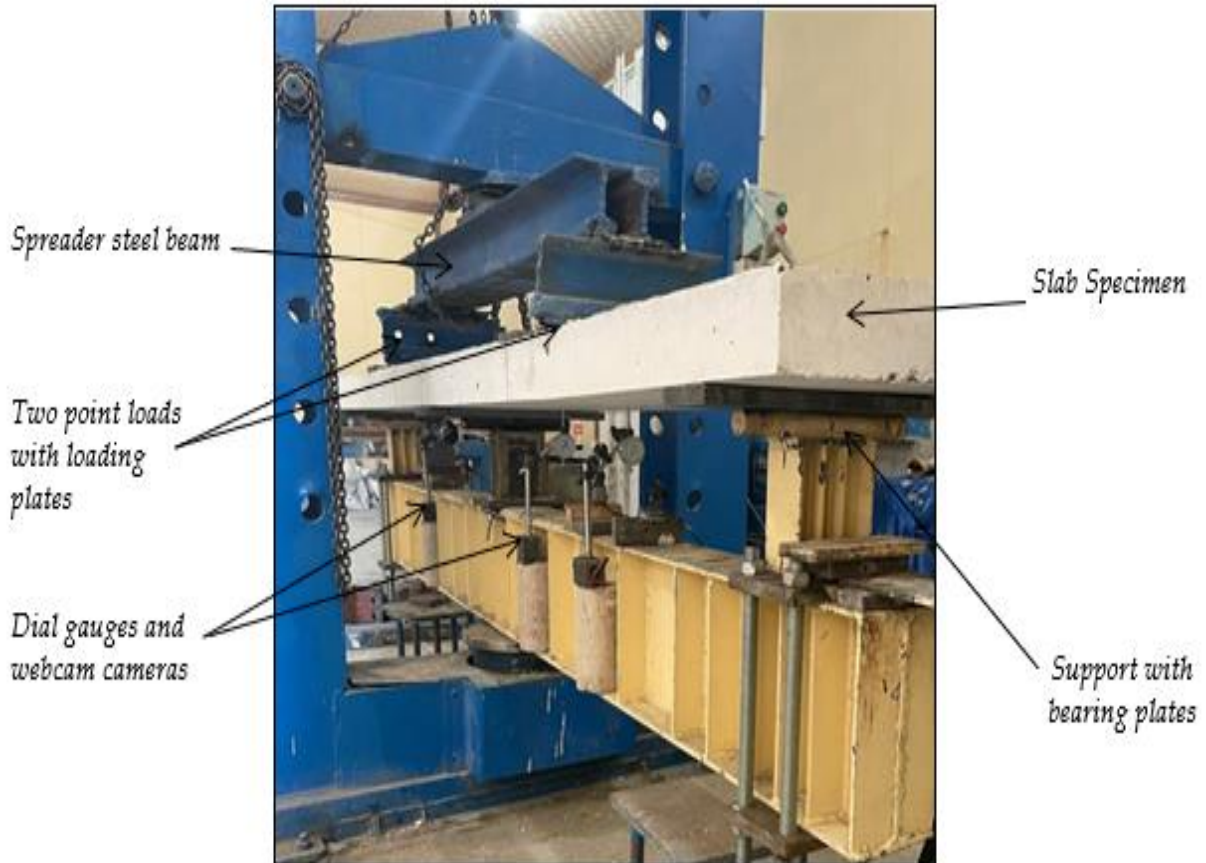


Figure 6. The universal testing machine and test configuration

The load was applied in phases from zero to the final load. The applied load was raised by 20% of the intended ultimate load for each slab at each stage. As a result, the first stage was initiated from zero to 10% of the designed ultimate load, then back to zero, and the loading procedure was repeated five times. Up to 20% of the designed ultimate load was applied in the second stage. Up to 30% of the designed ultimate load was used in the next step. Each step was repeated five times, with the fourth stage increasing to 40% and so on until failure (see Figure 7).

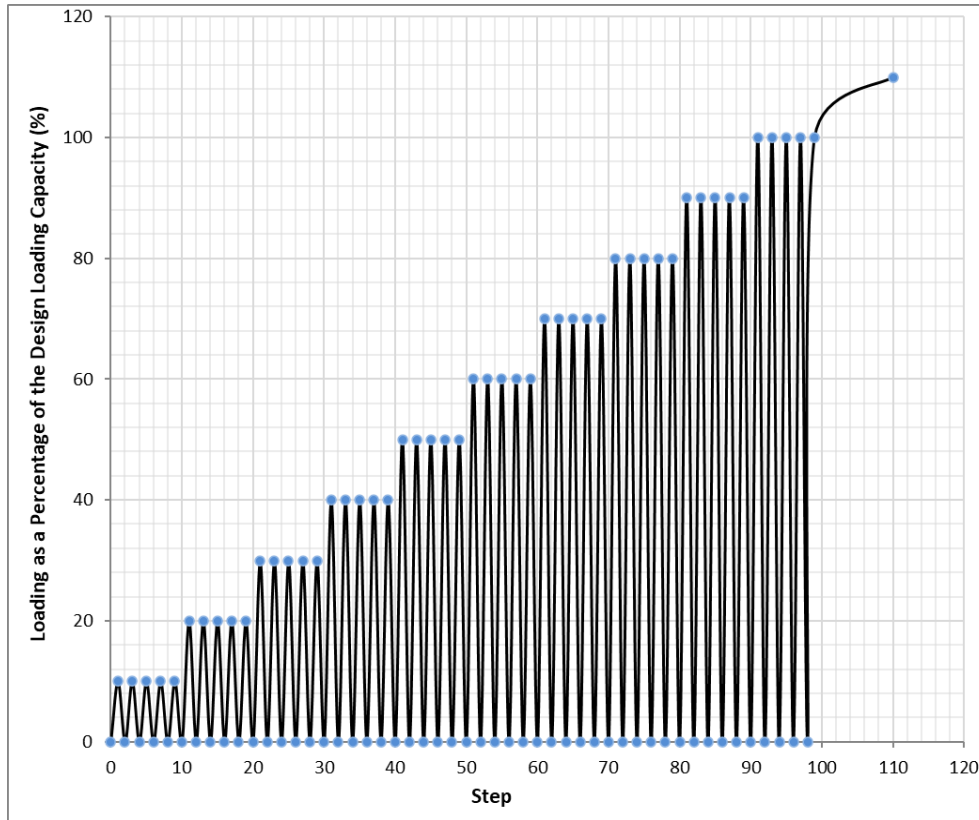


Figure 6. Loading protocol

4. Results and discussion

Table 2 summarizes the load capacity and failure mechanisms of the examined slabs.

Table 2. Summary of experimental results with failure mode

Specimen designation	Crack Loading		Failure Load (kN)	Deflection at service (mm)	Max deflection (mm)	Crack width at service (mm)	Failure mode
	Sagging region	Hogging region					
S1	5.75	5	41	4**	14.62	0.30	Flexural tension
S2	6.2	4	43	7.5**	23.9	0.30	Flexural tension
S3	5	7	39	6.5**	16.8	0.45	Flexural tension
S4	7	6	55	2.5	18	0.35	Flexural tension
S5	7.75	5.5	54	4**	21.2	0.38	Flexural tension
S6	6.5	8	54	3.3	19.32	0.50	Flexural tension

* Assumed service load = 60% from the ultimate load of each slab

** Did not satisfy the limitation of ACI 318 – 11 [18] ($\delta_{all} = 3.61$ mm)

The following sections cover the observation of specimens during the tests as well as comprehensive comments:

4.1. Load – Deflection response and ultimate loads

The mid-span deflection of slabs in this investigation was measured using a vertical dial gauge positioned in the centre of each span. Only the one that recorded the greatest deflection was included in the research to determine the span's load capacity. The load-midspan deflection curves for all the slabs evaluated in this investigation are shown in Figure 8. At the initial step of loading (no crack stage), there was generally negligible deflection. Figure 8 indicates that in the early stages of loading, all specimens exhibit a relatively small initial similar branch. In comparison to the prismatic slab, the deflection of the tapered slab increases as the applied load increases.

The load-deflection response of slabs with fixed end supports was stiffer than that of slabs with simple end supports, as predicted; nevertheless, prismatic slabs were stiffer than non-prismatic slabs in all support circumstances due to the presence of a negative moment. Thus, The flexural stiffness was altered, and the internal moment capacity was reduced, whether the reduction in slab thickness happened in the positive moment at the mid-span (negative haunch) or in the negative moment at the middle support (positive haunch).

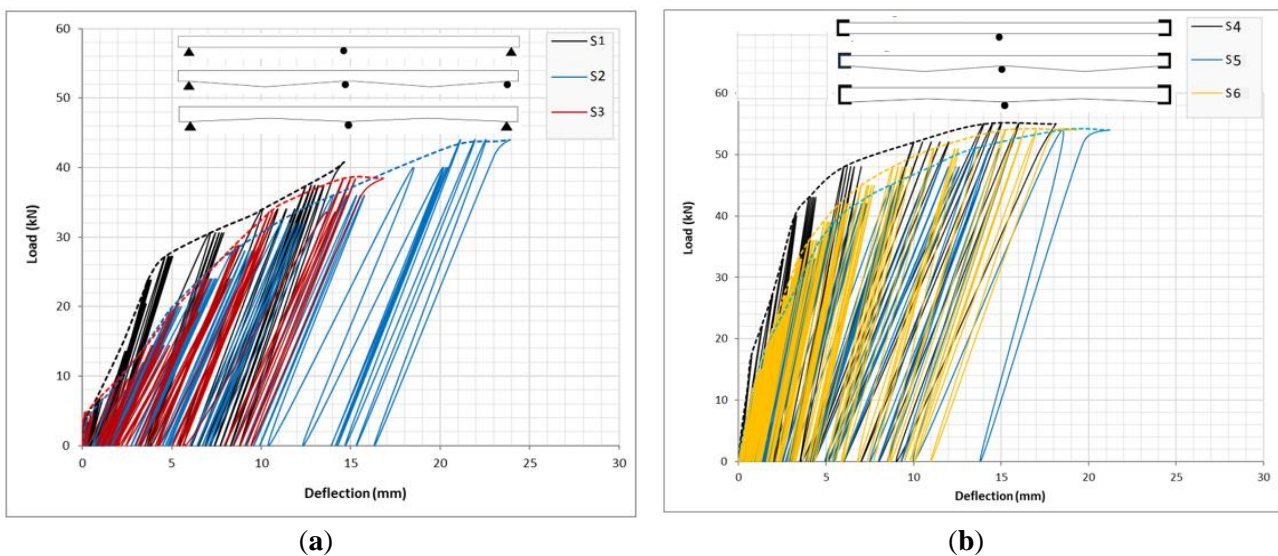


Figure 8. Experimental Load - Midspan deflection curves for slabs: (a) Effect of tapering configuration; (b) Effect of the support condition

It must be mentioned here that all slabs have the same span length, thus, the limitations of ACI 318-19 for immediate deflection due to maximum live load are the same for all slabs. The ultimate load capacity (P_u), the mid-span deflection at service load, and the mid-span deflection at ultimate loads for two-span slabs are presented in Table 2. In terms of support, it was discovered that employing fixed support at both ends in S4 specimens boosted ultimate load capacity in comparison to simply supported slabs. When compared to a prismatic slab, the tapered slab with a positive or negative haunch does not affect bearing capacity. It also generated a considerable increase in deflection at service load. The large increase in deflection under service load could be attributable to the reduction in slab thickness at critical sections (highest positive or negative moment), which gives the slabs a tapered form that influences their stiffness.

4.2. Cracking behavior and modes of failure

In the early stages of loading, reinforced concrete slabs are structurally sound. The first crack was seen in the tension face of the sagging or hogging region when the applied load reached the first cracking load, which was between 9% and 15% of the ultimate load. Following that, flexural cracks appeared and developed parallel to the crack, progressively spreading throughout the thickness of the slab.

When the magnitude of the load or the frequency of the repeated load increased, the stiffness of the slab models dropped (plastic stage). All of the specimens in this investigation failed in a flexural mode. This occurs after the tensile steel in the sagging and hogging regions was yielded, as demonstrated by the rapid growth in the breadth of certain cracks in these regions. Concrete was crushed at the top face of the specimen at the mid-span portion and the bottom face over the middle support when the tensile steel yielded.

Figure 9 shows photos of the control S4 specimen at failure.



Figure 9. Photos of the control S9 specimen at failure: (a) Failure of mid-span section (sagging region); (b) Failure of section over central support (hogging region)
 Observations of fracture development were done over the whole length of the slabs at each load level. Figure 10 shows the usual fracture patterns and failure causes found in simply and fixed supported slabs.



Figure 10. Typical Cracks pattern at failure for slabs of this study: (a) Cracks pattern for non-prismatic simply supported slab with positive haunch (S2 specimen); (b) Cracks pattern for non-prismatic fixed end support slab with positive haunch (S5 specimen)

Table 2 shows that as the slab depth grew so did the required load for producing the first fracture and vice versa. As a result, utilizing a non-prismatic slab with a negative haunch reduced the sagging zone's initial cracking stress while increasing it in the hogging region. This is because the concrete depth variation in the crucial section affects the moment of inertia and stiffness. For all slabs, the first crack width was determined to be almost 0.02 mm. According to Table 2, using a negative haunch for both types of support conditions resulted in a wider first crack at service load than the accepted limits of ACI 318-19 (0.4 mm).

4.3. Ductility

A structural member's ductility can be defined as the capacity of the member to withstand substantial deflection before failing. This feature is critical for structural elements subjected to seismic loads because it indicates failure before the incident, beyond yielding. Deflection ductility index (d) and energy absorption index (EAI) were two ductility definitions examined in this investigation. The energy absorption index is the ratio of the total area under the load-deflection curve to that under the elastic part only, while the deflection ductility index is the ratio of the deflection at the ultimate load of the slab to the deflection at yielding of the longitudinal tensile reinforcement (up to the yielding point). As a result, determining the load-deflection curve's yielding point is critical [19]. In the literature, there are several methods for estimating the yielding displacement. A technique originally presented by [20-23] is used in this investigation. As shown in Figure 11, y is the yield displacement of the corresponding elasto-plastic system with decreased stiffness calculated as the secant stiffness at 75% of the real system's ultimate load. Eq. 1 determines the deflection ductility index and Eq. 2 calculates the energy absorption index which are used in this research to represent this technique.

$$\text{Deflection ductility index, } \mu_d = \frac{\delta_u}{\delta_y} \text{ -----(1)}$$

$$\text{Energy absorption index, EAI} = \frac{A1+A2}{A1} \text{ -----(2)}$$

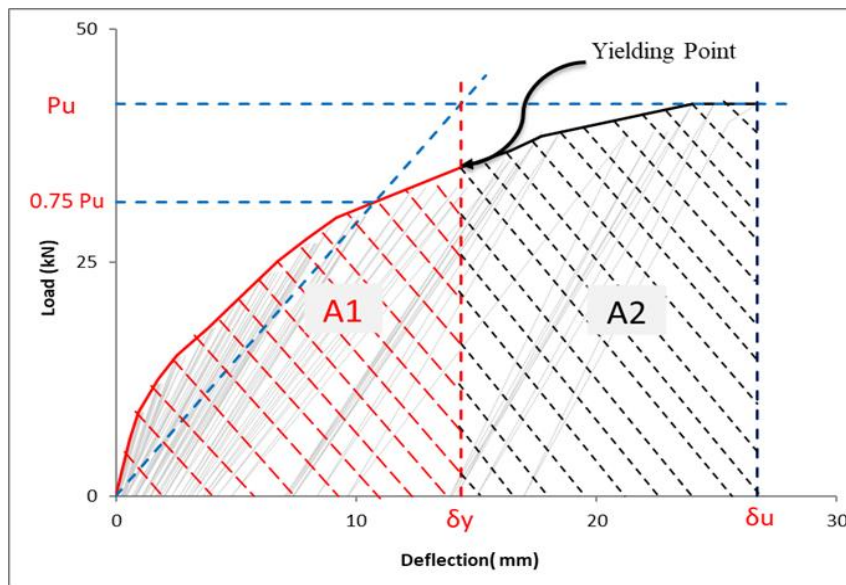


Figure 11. Typical diagram for determining the ductility index of RC slabs
The results of the deflection ductility index and energy absorption index with all the parameters that are required to determine them for slabs of this study are presented in Table 3.

Table 3. Ductility index for slabs

Beam designation	Yield deflection δ_y (mm)	Deflection at Ultimate load δ_u (mm)	Deflection ductility index μ_d	Elastic area A1 (kN.mm)	Plastic area A2 (kN.mm)	Total area A1+A2 (kN.mm)	Energy absorption index (EAI)
S6	9.5	14.62	1.53	217.5	189	406.5	1.86
S7	15.33	23.9	1.56	366	356	722	1.97
S8	11.33	16.8	1.48	230	204	434	1.88
S9	6.2	18	2.9	194	628	822	4.23
S10	8	21.2	2.65	237	670	907	3.8
S11	7	19.32	2.76	207	635	842	4.06

The predicted values of the energy absorption index for the corresponding tested specimens were practically identical to the deflection ductility index. It should be noted that using the tapered slab instead of the prismatic slab does not affect the ductility index. Besides, the higher ductility of fixed end specimens compared to simply support specimens could be attributed to the slab's higher stiffness during the first stage of loading, and vice versa at the plastic stage.

5. Conclusions

1. Because of their superior stiffness and almost equal load-carrying capability, prismatic continuous one-way slabs are preferred over non-prismatic ones.
2. Providing tapered slabs with positive or negative haunch has an insignificant effect on the bearing capacity with respect to prismatic slabs.
3. When compared to prismatic slab, providing tapered slab resulted in a considerable increase in deflection at service load. The reduction in slab thickness at the critical section (maximum positive or negative moment) by providing a tapered shape that impacts slab stiffness is linked to the large increase in deflection at service load.
4. The negative haunch caused an increase in the width of the first crack at service load more than the accepted limits of ACI 318-19.

5. Using a tapered slab instead of the prismatic slab has an insignificant effect on the ductility index.
6. Values of the energy absorption index were almost compatible with the deflection ductility index for the corresponding tested specimens.

Declaration of competing interest

The authors declare that they have no any known financial or non-financial competing interests in any material discussed in this paper.

Funding information

No funding was received from any financial organization to conduct this research.

References

- [1] Q. S. R. Marshdi, S. A. Hussien, B. M. Mareai, Z. S. Al-Khafaji, and A. A. Shubbar, "Applying of No-fines concretes as a porous concrete in different construction application," *Period Eng Nat Sci*, vol. 9, no. 4, pp. 999–1012, 2021.
- [2] A. A. Shubbar, Z. S. Al-khafaji, M. S. Nasr, and M. W. Falah, "USING NON-DESTRUCTIVE TESTS FOR EVALUATING FLYOVER FOOTBRIDGE: CASE STUDY."
- [3] Z. Al-Khafaji, A. A. Hafedh, N. K. Al-Bedyry, and S. A. Hussien, "Utilizing of shields factors for sedimentation movements and drainage channels at the middle of Iraq (as a case study)," *Period Eng Nat Sci*, vol. 10, no. 1, pp. 666–677, 2022.
- [4] H. G. Russell *et al.*, "State-of-the-art report on high-strength concrete," *ACI Comm*, vol. 363, p. 92, 1997.
- [5] M. A. Hamad *et al.*, "Production of Ultra-High-Performance Concrete with Low Energy Consumption and Carbon Footprint Using Supplementary Cementitious Materials Instead of Silica Fume: A Review," *Energies*, vol. 14, no. 24, p. 8291, 2021.
- [6] D. N. Jabbar, A. Al-Rifaie, A. M. Hussein, A. A. Shubbar, M. S. Nasr, and Z. S. Al-Khafaji, "Shear behaviour of reinforced concrete beams with small web openings," *Mater Today Proc*, 2021.
- [7] G. Balduzzi, M. Aminbaghai, E. Sacco, J. Füssl, J. Eberhardsteiner, and F. Auricchio, "Non-prismatic beams: a simple and effective Timoshenko-like model," *Int J Solids Struct*, vol. 90, pp. 236–250, 2016.
- [8] H. I. Archundia-Aranda and A. Tena-Colunga, "Cyclic behavior of reinforced concrete haunched beams failing in shear," in *Memorias, 14th World Conference on Earthquake Engineering, Beijing, China, Artículo*, 2008, no. 12–01, p. 105.
- [9] Y. Tayfur, A. Darby, T. Ibell, J. Orr, and M. Evernden, "Serviceability of non-prismatic concrete beams: Combined-interaction method," *Eng Struct*, vol. 191, pp. 766–774, 2019.
- [10] G. Zhang *et al.*, "Reinforced concrete deep beam shear strength capacity modelling using an integrative bio-inspired algorithm with an artificial intelligence model," *Eng Comput*, pp. 1–14, 2020.
- [11] A. Shubbar, M. Nasr, M. Falah, and Z. Al-Khafaji, "Towards net zero carbon economy: Improving the sustainability of existing industrial infrastructures in the UK," *Energies*, vol. 14, no. 18, p. 5896, 2021.
- [12] I. A. S. Al-shaarbaf, A. A. Ali, and M. A. Ahmed, "Experimental Behavior of Self Compacted Concrete Voids Slab Strips Under Repeated Loads," in *2019 12th International Conference on Developments in eSystems Engineering (DeSE)*, 2019, pp. 626–631.
- [13] S. Toshniwal, "Shear Analysis of Non-Prismatic Concrete Beams," 2019.
- [14] Z. S. Al-Khafaji and M. W. Falah, "Applications of high density concrete in preventing the impact of radiation on human health," *J Adv Res Dyn Control Syst*, vol. 12, no. 1 Special Issue, 2020, doi: 10.5373/JARDCS/V12SP1/20201115.
- [15] W. K. Tuama, M. M. Kadhum, N. A. Alwash, Z. S. Al-Khafaji, and M. S. Abduraheem, "RPC Effect of Crude Oil Products on the Mechanical Characteristics of Reactive-Powder and Normal-Strength Concrete," *Period Polytech Civ Eng*, 2020, doi: 10.3311/ppci.15580.
- [16] A. N. Abbas, H. K. Al-Naely, H. H. Abdulzahra, and Z. S. Al-Khafaji, "STRUCTURAL BEHAVIOR OF REINFORCED CONCRETE BEAMS HAVING CONSTRUCTION JOINT AT DIFFERENT ELEVATION."
- [17] H. M. Al-Baghdadi, A. A. F. Shubbar, and Z. S. Al-Khafaji, "The Impact of Rice Husks Ash on Some Mechanical Features of Reactive Powder Concrete with High Sulfate Content in Fine Aggregate," *Int Rev Civ Eng*, vol. 12, no. 4, pp. 248–254, 2021.
- [18] A. A. C. I. Standard, "Building Code Requirements for Structural Concrete (ACI 318-11)," 2011.
- [19] T. J. Sullivan, G. M. Calvi, and M. J. N. Priestley, "Initial stiffness versus secant stiffness in displacement

- based design,” in *13th World Conference of Earthquake Engineering (WCEE)*, 2004, no. 2888.
- [20] M. J. N. Priestley and R. Park, “Strength and ductility of concrete bridge columns under seismic loading,” *Struct J*, vol. 84, no. 1, pp. 61–76, 1987.
- [21] F. T. Al Rikabi, S. M. Sargand, H. H. Hussein, and I. Houry, "The Thermal Expansion of Synthetic Fiber-Reinforced Concrete under Air-Dry and Saturated Conditions," in *Congress on Technical Advancement 2017*, 2017, pp. 10-21.
- [22] R. Mutashar, S. Sargand, and I. Houry, "Influence of nonuniform box beam dimensions and bridge transverse slope on environmentally induced stresses in adjacent box beam bridges," *Journal of Performance of Constructed Facilities*, vol. 32, no. 6, p. 04018081, 2018.
- [23] S. M. Sargand, J. Kurdziel, and H. H. Hussein, "Thin-Walled Steel Fiber Reinforced Concrete Pipes Performance under Three-Edge Bearing Load," in *Pipelines 2018: Planning and Design*: American Society of Civil Engineers Reston, VA, 2018, pp. 355-363.